

# Validation of Model-Based Prognostics for Pneumatic Valves in a Demonstration Testbed

Chetan Kulkarni<sup>1</sup>, Matthew Daigle<sup>2</sup>, George Gorospe<sup>1</sup>, and Kai Goebel<sup>2</sup>

<sup>1</sup> *SGT, Inc., NASA Ames Research Center, Moffett Field, CA, 94035, USA*  
*chetan.s.kulkarni@nasa.gov*  
*george.gorospe@nasa.gov*

<sup>2</sup> *NASA Ames Research Center, Moffett Field, CA, 94035, USA*  
*matthew.j.daigle@nasa.gov*  
*kai.goebel@nasa.gov*

## ABSTRACT

Pneumatic-actuated valves play an important role in many applications, and for valves critical to the successful operation of the system, prognostics of these valves becomes extremely important and valuable. In order to facilitate the validation of prognostics algorithms for pneumatic valves, we have constructed a pneumatic valve testbed for use with a cryogenic propellant loading system. The testbed enables the injection of faults with a controllable fault progression profile. Specifically, we can introduce controllable pneumatic gas leaks, the most common faults associated with pneumatic valves. We focus on a valve that moves discretely between open and closed, and is controlled through a solenoid valve. In this paper, we apply a model-based prognostics approach for pneumatic valves on the testbed. We demonstrate the approach using real experimental data obtained from the testbed.

## 1. INTRODUCTION

Pneumatic-actuated valves play a critical role in many systems. For example, they are used to control the flow of propellant in cryogenic propellant loading systems, and failures can have an adverse impact on system safety and launch availability (Daigle & Goebel, 2011a). This motivates the need for valve health monitoring and prognosis. To facilitate the maturation of prognostics technology, testbeds can be constructed that allow for fault injection with controllable fault progression profiles, which have been developed for electrical power systems (Poll, Patterson-Hine, Camisa, Garcia, et al., 2007; Poll, Patterson-Hine, Camisa, Nishikawa, et al., 2007), electromechanical actuators (Balaban et al., 2010), and mobile robots (Tang, Hettler, Zhang, & DeCastro, 2011; Bala-

ban et al., 2013). For the purpose of maturing and validating valve prognostics approaches, we have developed a pneumatic valve testbed (Kulkarni, Daigle, & Goebel, 2013).

Whereas earlier work on valve prognosis used algorithms centered on particle filters (Daigle & Goebel, 2011a, 2011b, 2010), in this paper we use a new model-based method based on the measurement of valve open and close times, recently developed in (Daigle, Kulkarni, & Gorospe, 2014). In real valve operations, typically only valve position is measured, from which the only meaningful information for prognostics is valve open and close times. The new approach is therefore much simpler and requires significantly less computation to isolate and identify faults, and predict end of life (EOL) and remaining useful life (RUL). The approach still follows the general estimation-prediction framework developed in the literature for model-based prognostics (Orchard & Vachtsevanos, 2009; Daigle & Goebel, 2013). In (Daigle et al., 2014), the approach was demonstrated in simulation; in this paper, we apply the approach using real data from the pneumatic valve testbed.

The structure of the paper is as follows. Section 2 discusses the overall setup of the valve prognostics testbed. Section 3 presents the valve model. Section 4 provides the valve prognosis framework, and Section 5 presents prognosis results using testbed data. Section 6 concludes the paper.

## 2. VALVE TESTBED

The valve prognostics testbed, shown in Fig. 1, has been developed to demonstrate valve prognosis in the context of cryogenic refueling operations (Kulkarni et al., 2013). The dashed lines denote the electrical signals, including the data acquisition I/O signals, power lines, etc. The solid lines denote the pneumatic pressure lines connecting the supply and the valves. Power is provided by both a typical power supply

Chetan Kulkarni et al. This is an open-access article distributed under the terms of the Creative Commons Attribution 3.0 United States License, which permits unrestricted use, distribution, and reproduction in any medium, provided the original author and source are credited.

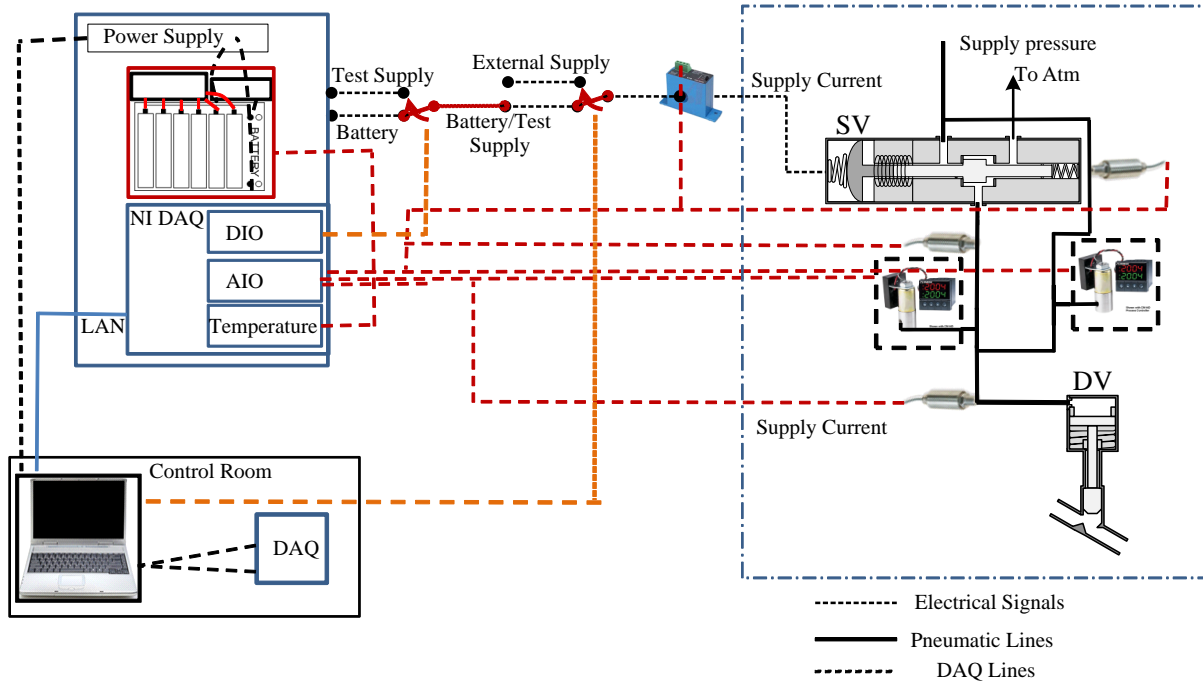


Figure 1. Prognostics demonstration testbed schematic.

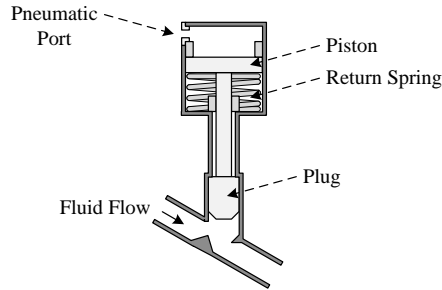


Figure 2. Discrete-controlled valve.

and a battery backup supply, and includes a fail-safe mode to isolate the valve prognostics testbed from the cryogenic loading system it may interface with.

The testbed includes a discrete-controlled valve (DV), illustrated in Fig. 2, which is a normally-open valve with a linear cylinder actuator. The valve is closed by filling the chamber above the piston with gas up to the supply pressure, and opened by evacuating the chamber to atmosphere, with the spring returning the valve to its default position.

A three-way two-position solenoid valve (SV), illustrated in Fig. 3, is used for controlling the operation of the DV valve. The cylinder port connects to the valve, the normally closed (NC) port connects to the supply pressure, and normally open (NO) port is left unconnected, allowing venting to atmosphere. When the solenoid is energized, the path from the NC port to cylinder port is open, allowing gas to pass from

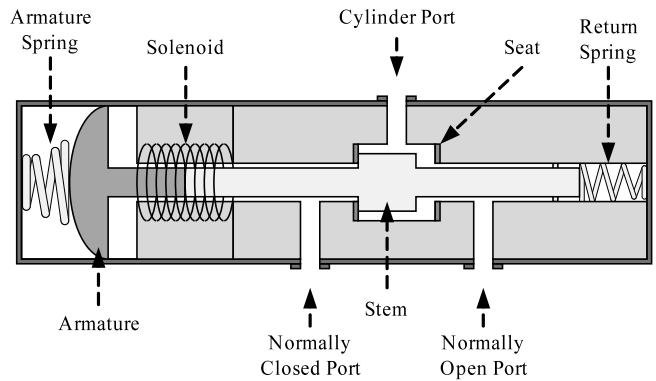


Figure 3. Three-way two-position solenoid valve.

the supply to the valve, thus actuating the valve. When deenergized, the supply pressure is closed off and the path from the cylinder port to the NO port is opened, thus venting the actuation pressure in the DV valve, allowing the valve to open due to the return spring. The solenoid is powered by 24 V DC either through the power supply or the batteries.

The data from the different sensors is collected using an 8-slot NI cDAQ-9188 Gigabit Ethernet chassis as the data acquisition (DAQ) system that is designed for remote or distributed sensor measurements. For the testbed, control and data acquisition must be done remotely to meet safety requirements. A single NI CompactDAQ chassis can measure up to 256 channels of sensor signals, analog I/O (AIO), digital I/O (DIO), and counter/timers with an Ethernet interface back

to a host machine. All the operations for the cDAQ-9188 are controlled through an interface designed in LabVIEW. Additional details of the testbed and data acquisition system are described in (Kulkarni et al., 2013).

In this work, we focus on faults affecting the DV. Pneumatic valves can suffer from leaks, an increase in friction due to wear, and spring degradation (Daigle & Goebel, 2011a). Because friction and spring faults cannot be injected or their rate of progression controlled, we are limited only to leak faults, however, leaks are the most common faults found in pneumatic valves. In the configuration shown in Fig. 1, two different leak faults may be considered: (i) a leak to atmosphere, and (ii) a leak from the supply. In the former, this can manifest as a leak across the NO seat of the solenoid valve, or a leak in the pressure line going to the pneumatic valve. In the latter case, the fault can manifest as a leak across the NC seat of the solenoid valve. To emulate these faults, we installed two remotely-operated proportional valves, as shown in Fig. 1. One valve leaks to atmosphere (henceforth called the vent valve), while the other is installed on a bypass line around the solenoid valve (henceforth called the bypass valve).

The position of the vent and bypass valves can be controlled through a current signal, continuous between 0 and 100% open. In this way, we can control the fault progression (growth of leak size) according to various progression profiles.

Fig. 4 illustrates a leak to atmosphere using the vent valve (V1). The leak through V1 emulates a leak at the cylinder port or across the NO seat. Similarly, Fig. 5 illustrates a leak from the supply using the bypass valve (V2). The leak through V2 emulates a leak across the NC seat. The effect of these faults on valve behavior is described in Section 3.

### 3. VALVE MODELING

In the following, we present the model using continuous-time. For implementation purposes, we convert to a discrete-time version using a sample time of  $1 \times 10^{-3}$  s. This model was originally presented in (Daigle et al., 2014), and we summarize it here for completeness.

We develop a physics model of the valve based on mass and energy balances. The system state includes the position of the valve,  $x(t)$ , the velocity of the valve,  $v(t)$ , the mass of the gas in the volume above the piston, and the mass of the gas in the pipe connecting the solenoid valve to the pneumatic valve port:

$$\mathbf{x}(t) = [x(t) \quad v(t) \quad m_t(t) \quad m_p(t)]^T. \quad (1)$$

The position is defined as  $x = 0$  when the valve is fully closed, and  $x = L_s$  when fully open, where  $L_s$  is the stroke length of the valve.

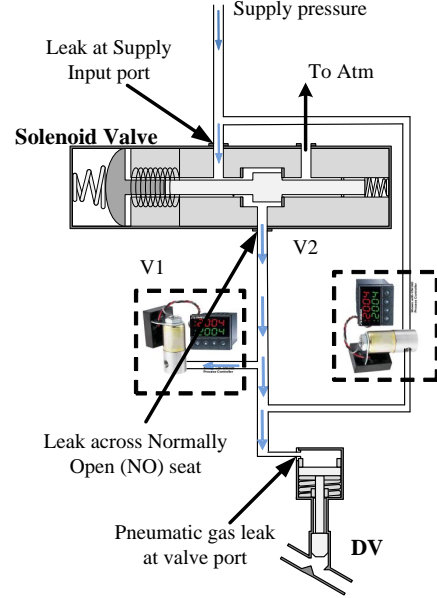


Figure 4. Solenoid valve leak fault injection when energized on DV valve.

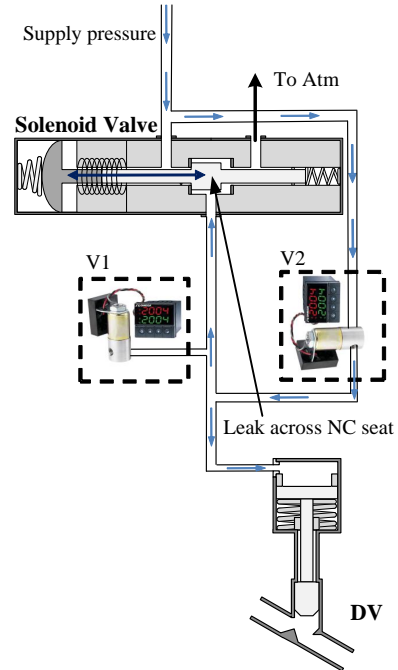


Figure 5. Solenoid valve leak fault injection when de-energized on DV valve.

The derivatives of the states are described by

$$\dot{\mathbf{x}}(t) = [v(t) \quad a(t) \quad f_t(t) \quad f_p(t)]^T, \quad (2)$$

where  $a(t)$  is the valve acceleration,  $f_t(t)$  is the mass flow going into the pneumatic port from the pipe, and  $f_p(t)$  is the total mass flow into the pipe.

The single input is considered to be

$$\mathbf{u}(t) = [u_t(t)], \quad (3)$$

where  $u_t(t)$  is input pressure to the pneumatic port, which alternates between the supply pressure and atmospheric pressure depending on the commanded valve position.

The acceleration is defined by the combined mass of the piston and plug,  $m$ , and the sum of forces acting on the valve, which includes the force from the pneumatic gas,  $F_p = (p_t(t) - p_{atm})A_p$ , where  $p_t(t)$  is the gas pressures on the top of the piston, and  $A_p$  is the surface area of the piston; the weight of the moving parts of the valve,  $F_w = -mg$ , where  $g$  is the acceleration due to gravity; the spring force,  $F_s = k(x(t) + x_o)$ , where  $k$  is the spring constant and  $x_o$  is the amount of spring compression when the valve is open; friction,  $F_f = -rv(t)$ , where  $r$  is the coefficient of kinetic friction, and the contact forces  $F_c(t)$  at the boundaries of the valve motion,

$$F_c(t) = \begin{cases} k_c(-x), & \text{if } x < 0, \\ 0, & \text{if } 0 \leq x \leq L_s, \\ -k_c(x - L_s), & \text{if } x > L_s, \end{cases} \quad (4)$$

where  $k_c$  is the (large) spring constant associated with the flexible seals. Overall, the acceleration term is defined by

$$a(t) = \frac{1}{m}(F_s - F_p - F_f - F_w + F_c). \quad (5)$$

The pressure  $p_t(t)$  and the pipe pressure,  $p_p(t)$ , are calculated as:

$$p_t(t) = \frac{m_t(t)R_gT}{V_{t_0} + A_p(L_s - x(t))}p_p(t) = \frac{m_p(t)R_gT}{V_p} \quad (6)$$

where we assume an isothermal process in which the (ideal) gas temperature is constant at  $T$ ,  $R_g$  is the gas constant for the pneumatic gas,  $V_{t_0}$  is the minimum gas volume for the gas chamber above the piston, and  $V_p$  is the pipe volume.

The gas flows are given by:

$$f_{p,in}(t) = f_g(u_t(t), p_p(t)) \quad (7)$$

$$f_{p,leak}(t) = f_g(p_p(t), p_{leak}) \quad (8)$$

$$f_{p,t}(t) = f_g(p_p(t), p_t(t)) \quad (9)$$

$$f_p(t) = f_{p,in}(t) - f_{p,t}(t) - f_{p,leak}(t) \quad (10)$$

$$f_t(t) = f_{p,t}(t) \quad (11)$$

where  $f_{p,in}$  is the flow into the pipe from the supply or atmosphere,  $f_{p,leak}$  is a leak term with  $p_{leak}$  being the pressure outside the leak,  $f_{p,t}$  is the flow from the pipe to the chamber above the piston, and  $f_g$  defines gas flow through an orifice for choked and non-choked flow conditions (Perry & Green, 2007). Non-choked flow for  $p_1 \geq p_2$  is given by

$$f_{g,nc}(p_1, p_2) = C_s A_s p_1 \sqrt{\frac{\gamma}{Z R_g T} \left( \frac{2}{\gamma - 1} \right) \left( \left( \frac{p_2}{p_1} \right)^{\frac{2}{\gamma}} - \left( \frac{p_2}{p_1} \right)^{\frac{\gamma+1}{\gamma}} \right)}, \quad (12)$$

where  $\gamma$  is the ratio of specific heats,  $Z$  is the gas compressibility factor,  $C_s$  is the flow coefficient, and  $A_s$  is the orifice area. Choked flow for  $p_1 \geq p_2$  is given by

$$f_{g,c}(p_1, p_2) = C_s A_s p_1 \sqrt{\frac{\gamma}{Z R_g T} \left( \frac{2}{\gamma + 1} \right)^{\frac{\gamma+1}{\gamma-1}}}. \quad (13)$$

Choked flow occurs when the upstream to downstream pressure ratio exceeds  $\left( \frac{\gamma+1}{2} \right)^{\gamma/(\gamma-1)}$ . The overall gas flow equation is then given by

$$f_g(p_1, p_2) = \begin{cases} f_{g,nc}(p_1, p_2) & \text{if } p_1 \geq p_2 \\ & \text{and } \frac{p_1}{p_2} < \left( \frac{\gamma+1}{2} \right)^{\frac{\gamma}{\gamma-1}}, \\ f_{g,c}(p_1, p_2) & \text{if } p_1 \geq p_2 \\ & \text{and } \frac{p_1}{p_2} \geq \left( \frac{\gamma+1}{2} \right)^{\frac{\gamma}{\gamma-1}}, \\ -f_{g,nc}(p_2, p_1) & \text{if } p_2 > p_1 \\ & \text{and } \frac{p_2}{p_1} < \left( \frac{\gamma+1}{2} \right)^{\frac{\gamma}{\gamma-1}}, \\ -f_{g,c}(p_2, p_1) & \text{if } p_2 > p_1 \\ & \text{and } \frac{p_2}{p_1} \geq \left( \frac{\gamma+1}{2} \right)^{\frac{\gamma}{\gamma-1}}, \end{cases} \quad (14)$$

The only available measurement is the valve position, so we have

$$\mathbf{y}(t) = [x(t)]. \quad (15)$$

Fig. 6 shows an example nominal valve cycle. The valve starts in its default open state. The valve is commanded to close at 0 s. Supply pressure (75 psig) is delivered to the pipe and to the valve, causing the piston to lower, closing the valve just after 1 s. At 4 s, the valve is commanded to open, and the pipe is opened to atmosphere. The pipe pressure and valve pressure drop, and once the pressure drops low enough, the spring overcomes the pressure force and the piston moves upwards. The valve completes opening just after 6 s. The valve parameters were identified from known valve specifications, and unknown parameters estimated to match the nominal opening and closing times, which for the actual valve, are both around 3.5 s.

As discussed in Section 2, we consider two different leak faults, one in which there is a leak from the supply pressure input to the valve ( $p_{leak}$  is the supply pressure), emulated using the bypass valve, and one in which there is a leak out to atmosphere ( $p_{leak}$  is atmospheric pressure), emulated using

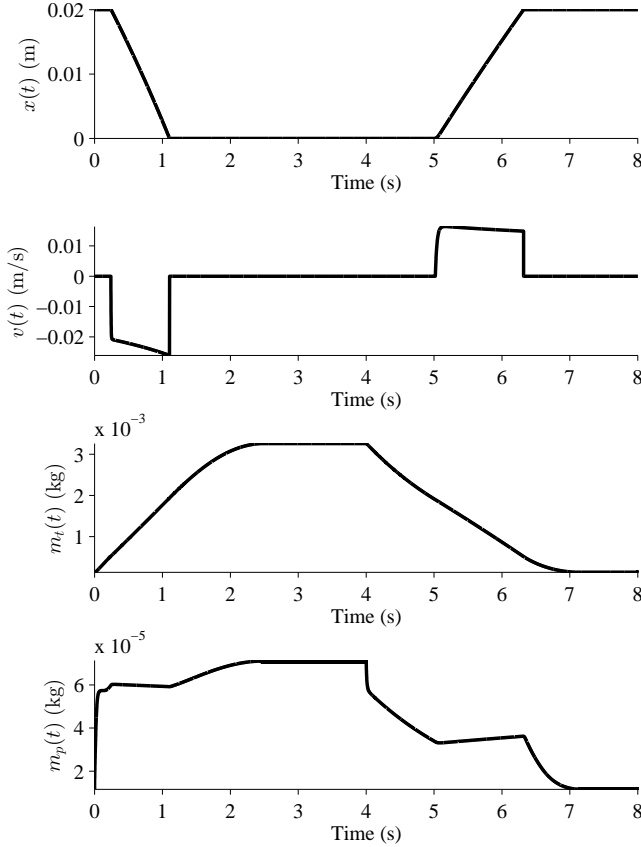


Figure 6. Nominal valve operation.

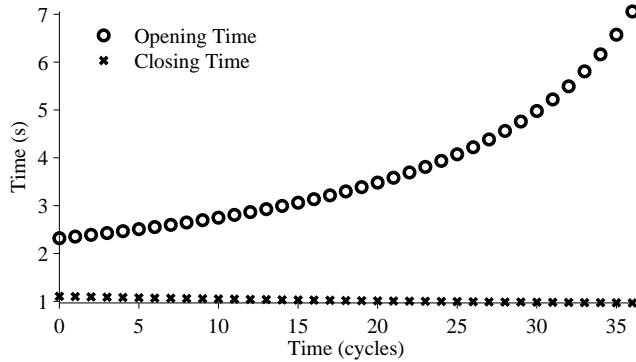


Figure 7. Valve timing with leak from supply, with linearly increasing leak area.

the vent valve. In the former case, the valve will close more slowly and open faster, and in the latter, the valve will open more slowly and close faster. With a large enough leak, the valve may fail to open or close completely. Fig. 7 shows the changes in valve timing with the leak from the supply, and Fig. 8 shows the changes in valve timing with the leak to atmosphere. Here, we consider a damage progression model where the leak hole area increases linearly with time.

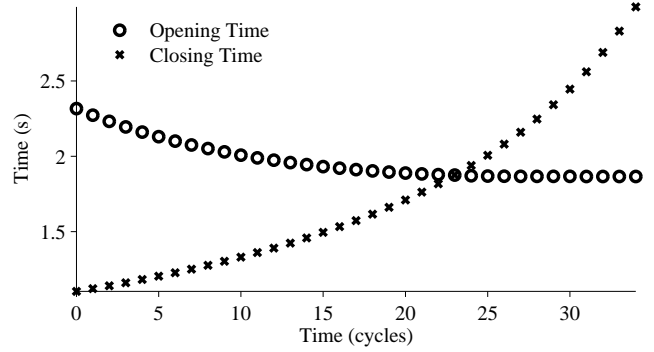


Figure 8. Valve timing with leak to atmosphere, with linearly increasing leak area.

In the testbed, we cannot control the leak area, but only the leak valve position, which varies nonlinearly with the effective leak area. So, unlike in (Daigle et al., 2014), we must consider also this relationship, so that we can map from open/close times to leak size to leak valve position, for which we assume a particular damage progression profile. The relationship between the leak valve position and its effective area is a function of the valve flow coefficient, which is nonlinear. In this case, we assume that the effective area is equal to the product of the square of the position ( $A_{leak}^2$ ) and a conversion coefficient.

$$kA_{leak}^2 = C_{leak} \quad (16)$$

We define valve end of life (EOL) through open/close time limits of the valves, as in real valve operations (Daigle & Goebel, 2011a). The valve in the testbed is required to open within 7 s and close within 6 s.

#### 4. VALVE PROGNOSIS

We describe in this section the prognosis framework developed for the valve, following the general estimation-prediction framework of model-based prognostics (Luo, Patipati, Qiao, & Chigusa, 2008; Orchard & Vachtsevanos, 2009; Daigle & Goebel, 2013). However, since we use only valve timing values for prognosis, we use a simpler estimation approach (Daigle et al., 2014), similar to that developed in (Teubert & Daigle, 2013), as opposed to more complex and computationally intensive filtering approaches used in previous works. We first formulate the prognostics problem, followed by a description of the estimation approach and a description of the prediction approach.

#### 4.1. Problem Formulation

We assume the system model may be generally defined as

$$\mathbf{x}(k+1) = \mathbf{f}(k, \mathbf{x}(k), \boldsymbol{\theta}(k), \mathbf{u}(k), \mathbf{v}(k)), \quad (17)$$

$$\mathbf{y}(k) = \mathbf{h}(k, \mathbf{x}(k), \boldsymbol{\theta}(k), \mathbf{u}(k), \mathbf{n}(k)), \quad (18)$$

where  $k$  is the discrete time variable,  $\mathbf{x}(k) \in \mathbb{R}^{n_x}$  is the state vector,  $\boldsymbol{\theta}(k) \in \mathbb{R}^{n_\theta}$  is the unknown parameter vector,  $\mathbf{u}(k) \in \mathbb{R}^{n_u}$  is the input vector,  $\mathbf{v}(k) \in \mathbb{R}^{n_v}$  is the process noise vector,  $\mathbf{f}$  is the state equation,  $\mathbf{y}(k) \in \mathbb{R}^{n_y}$  is the output vector,  $\mathbf{n}(k) \in \mathbb{R}^{n_n}$  is the measurement noise vector, and  $\mathbf{h}$  is the output equation.<sup>1</sup>

In prognostics, we are interested in predicting the occurrence of some event  $E$  that is defined with respect to the states, parameters, and inputs of the system. We define the event as the earliest instant that some event threshold  $T_E : \mathbb{R}^{n_x} \times \mathbb{R}^{n_\theta} \times \mathbb{R}^{n_u} \rightarrow \mathbb{B}$ , where  $\mathbb{B} \triangleq \{0, 1\}$  changes from the value 0 to 1 (Daigle & Sankararaman, 2013). That is, the time of the event  $k_E$  at some time of prediction  $k_P$  is defined as

$$k_E(k_P) \triangleq \inf\{k \in \mathbb{N} : k \geq k_P \wedge T_E(\mathbf{x}(k), \boldsymbol{\theta}(k), \mathbf{u}(k)) = 1\}. \quad (19)$$

The time remaining until that event,  $\Delta k_E$ , is defined as

$$\Delta k_E(k_P) \triangleq k_E(k_P) - k_P. \quad (20)$$

In the context of systems health management,  $T_E$  is defined via a set of performance constraints that define what the acceptable states of the system are, based on  $\mathbf{x}(k)$ ,  $\boldsymbol{\theta}(k)$ , and  $\mathbf{u}(k)$  (Daigle & Goebel, 2013). In this context,  $k_E$  represents end of life (EOL), and  $\Delta k_E$  represents remaining useful life (RUL). For valves, timing requirements are provided that define the maximum allowable time a valve may take to open or close, and these define  $T_{EOL}$  (Daigle & Goebel, 2011a).

The prognostics problem is to compute estimates of EOL and/or RUL. To do this, we first perform an estimation step that computes estimates of  $\mathbf{x}(k)$  and  $\boldsymbol{\theta}(k)$ , followed by a prediction step that computes EOL/RUL using these values as initial states. For the case of the valve, the future inputs are known, i.e., the valve is simply cycled open and closed, so there is no uncertainty with respect to future inputs.

#### 4.2. Estimation

Since only valve position is measured, only valve timing values are useful for prognostics. We can obtain this information from the continuous position measurement data by extracting and computing the difference in time between when the valve is commanded to move, and when it reaches its final position. Using the model, we can map this time to the fault size that corresponds to it. In order to obtain this result quickly, we

compute a lookup table that maps leak size to corresponding open and close times, by simulating the model given different leak sizes in the expected ranges. A similar approach is used for current-pressure transducers in (Teubert & Daigle, 2013).

We are interested in mapping this leak size back to the position of the leak valve, which we assume is increasing linearly. For this, we simply take the square root (Eq. 16). Since this transformed value is progressing linearly, we will essentially be estimating the gain term  $k$ , lumped with the slope of the leak valve position. So, given the estimated values of damage progression, we can perform a regression to find the line that fits this data, using the last  $N$  cycles.

For the leak to atmosphere, only closing times can be used (Daigle et al., 2014). This is because, in the presence of this leak, the valve may not get up to the full supply pressure when the valve closes in time for the next cycle, so since the internal valve actuator pressure is not measured, we do not have a correct initial condition for the simulation with which to estimate the leak parameter value for the following opening time. For the supply leak, we have analogous situation and can use only opening times for leak parameter estimation.

#### 4.3. Prediction

Given the current estimated leak parameter value, and the regression parameters, we can compute the value of the leak parameter at any future time, defining the damage progression equation. Using the lookup table, we can map the maximum valve open/close times to maximum leak parameter values for the two leak faults, and this defines the EOL thresholds in the leak parameter space. Using the relationship between leak size and leak valve position, we can then obtain corresponding maximum values here, and then solve for the time at which that threshold is crossed, given the fitted line, and thus obtain EOL.

Prediction is not performed until a fault is detected. To detect faults, we use a threshold on the opening times and closing times. If the mean valve opening or closing time, averaged over the last 3 cycles, is over the threshold, then a fault is detected. The regression is performed only over the data obtained since fault detection, so that nominal valve behavior is not used to estimate the fault progression parameters. The use of a filter on the data for fault detection introduces a slight lag, however in practice fault progression is very slow so this lag is negligible relative to the true EOL. In general, more robust fault detection strategies may also be used, but for our purposes a simple threshold works well.

We can isolate which fault is present by inspecting open/close timing trends (see Fig. 8 and Fig. 7). Since the two faults produce different qualitative changes on the valve timing, the observed trends tell us which fault is actually present.

<sup>1</sup>Bold typeface denotes vectors, and  $n_a$  denotes the length of a vector  $\mathbf{a}$ .

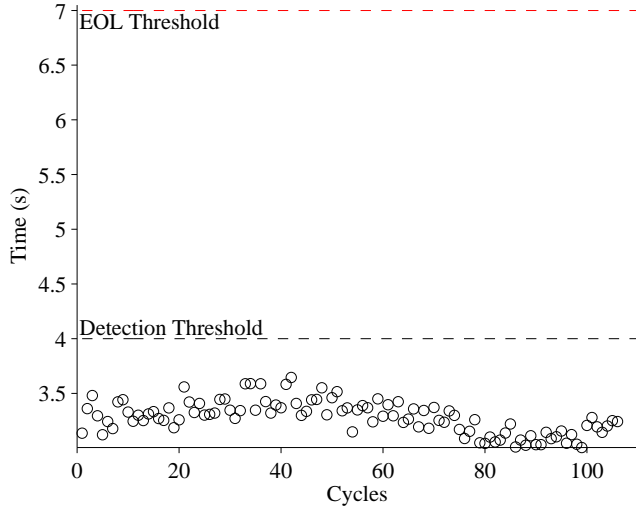


Figure 9. Valve open times with an atmospheric leak.

## 5. RESULTS

We present here experimental results using the valve prognostics testbed. In each experiment, the valve is cycled open and closed repeatedly, every 10 s, until the end of life condition is reached. For the valve under consideration, the valve is considered to be failed when it opens in 7 s or greater, or closes in 6 s or greater. Fault detection thresholds of 4 s and 3.6 s are used for the open and close times, respectively. The fault is injected by linearly increasing the open percentage of the desired leak valve in increments of 1%. We first present results for the leak to atmosphere fault, followed by results for the leak from supply fault.

### 5.1. Leak to Atmosphere

As described in Section 2, the leak to atmosphere fault is injected by controlling the position of the leak valve V1. This emulates a leak across the NO seat of the solenoid valve, or a leak on the gas line going to the pneumatic valve. As described in Section 3, this fault causes a decrease in opening times and an increase in closing times. Fig. 9 shows the open times of the valve during the fault progression, and Fig. 10 shows the close times. It is difficult to determine a trend in the open times, and they do not cross the detection threshold. The close times are very noisy, and do cross the closing time threshold at the 48th cycle. Based on the open and close times, the fault must be a leak to atmosphere, in agreement with the model.

The estimated leak parameter values, based on the close times of the DV, are shown in Fig. 11. In order to estimate the fault progression parameters, the last 50 values are used. Since the close times are quite noisy, a larger window is needed for this purpose. The RUL predictions are given in Fig. 12, where  $\alpha = 0.3$  represents a desired accuracy constraint, and

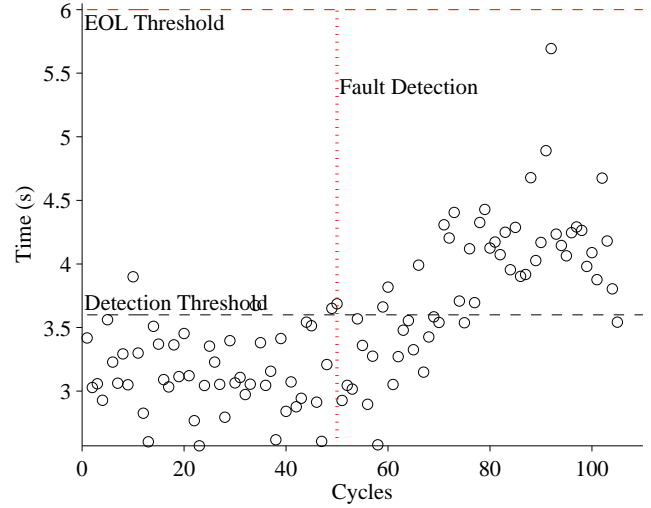


Figure 10. Valve close times with an atmospheric leak.

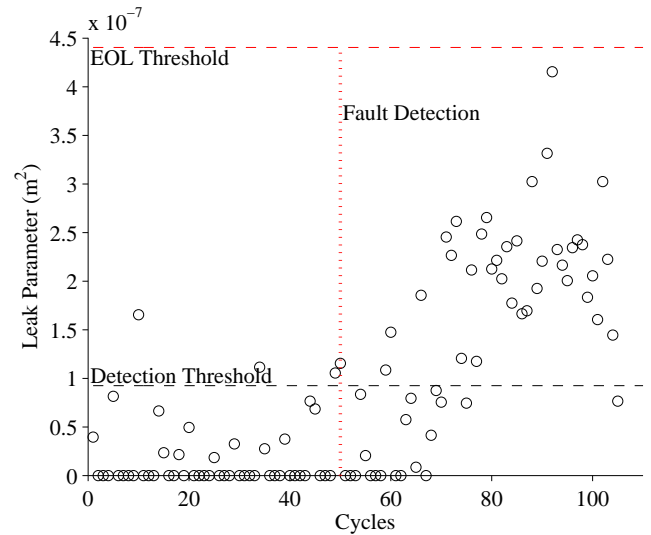


Figure 11. Estimated leak parameter values based on valve closing times for the atmospheric leak

$RUL^*$  denotes the true RUL. The predictions converge relatively quickly after the fault is detected. The algorithm predicts the RUL values within the  $\alpha$ -cone, until cycle 100. After that point, the close times have more spread, as can be seen from Fig. 10. Due to this, the algorithm overestimates the RUL values towards the end of the experiment.

### 5.2. Leak from Supply

As described in Section 2, the leak from supply fault is injected by controlling the position of the leak valve V2. This emulates a leak across the NC seat of the solenoid valve. As described in Section 3, this fault causes an increase in opening times and a slight decrease in closing times. Fig. 13 shows the open times of the valve during the fault progression, and

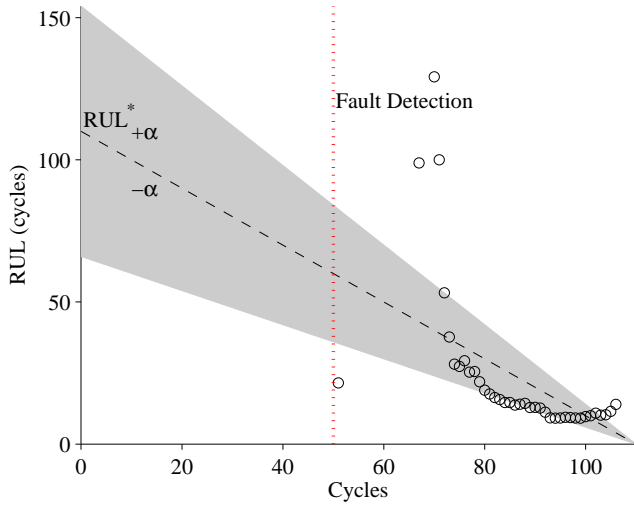


Figure 12. Predicted RUL values for the atmospheric leak.

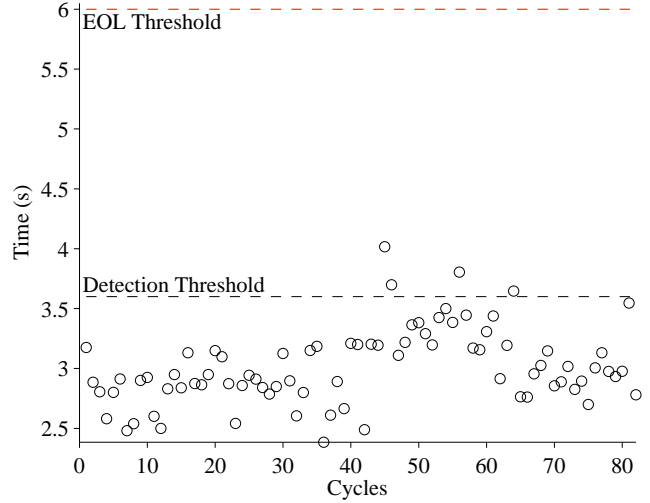


Figure 14. Valve close times with a leak from supply.

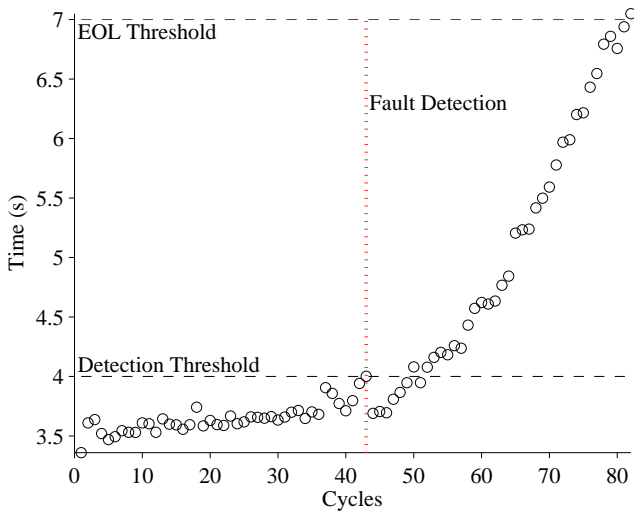


Figure 13. Valve open times with a leak from supply.

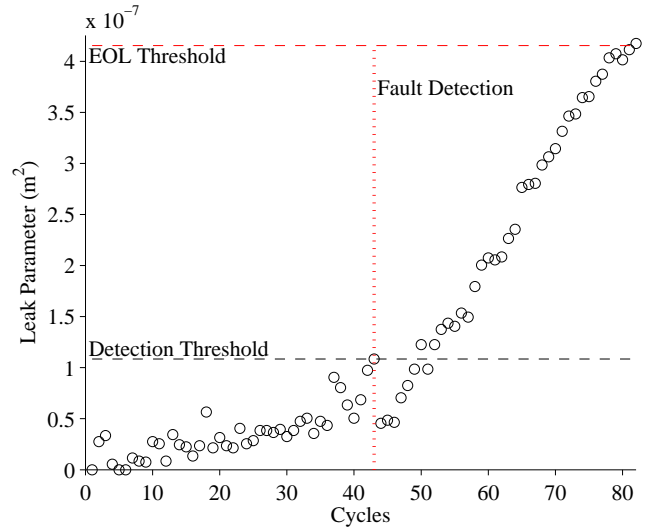


Figure 15. Estimated leak parameter values based on valve opening times for the leak from supply.

Fig. 14 shows the close times. The observed trends are in agreement with the model. A fault is detected at the 43rd cycle based on the opening times.

Fig. 15 shows the estimated leak parameters, and Fig. 16 shows the RUL predictions. After detecting the fault the predictions converge occurs relatively quickly. Because the opening times are less noisy, only the past 15 cycles are used to determine the fault progression parameters, and this improves convergence. After entering the  $\alpha$ -cone, the predictions for remain until EOL.

For further validation, we present a second experiment for a leak from the supply. The experiment is performed exactly the same, however, performance variations exist from one experiment to the next, and we must ensure that our approach is robust to those variations. The open and close times for this

experiment are similar to the previous experiment, with some variations. In this case, the fault is detected later at around the 47th cycle in the opening times. The RUL predictions for this experiment are shown in Fig. 17. Although the valve timing is slightly different, the RUL predictions are just as accurate, and, in fact, a little more so in this case.

## 6. CONCLUSIONS

In this paper, we described a testbed for injecting faults in pneumatic valves. We developed a model of the valve including leak faults, and presented a valve prognosis framework that operates with limited measurements, using only valve timing information for prognosis. We demonstrated the prognosis framework with experimental data from the testbed for



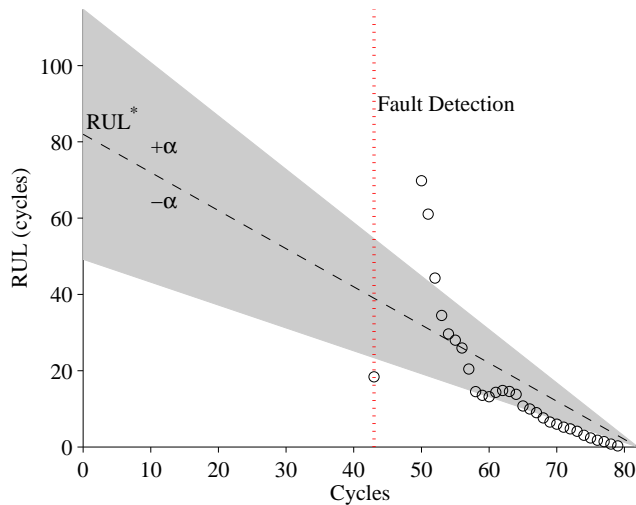


Figure 16. Predicted RUL values for the leak from supply.

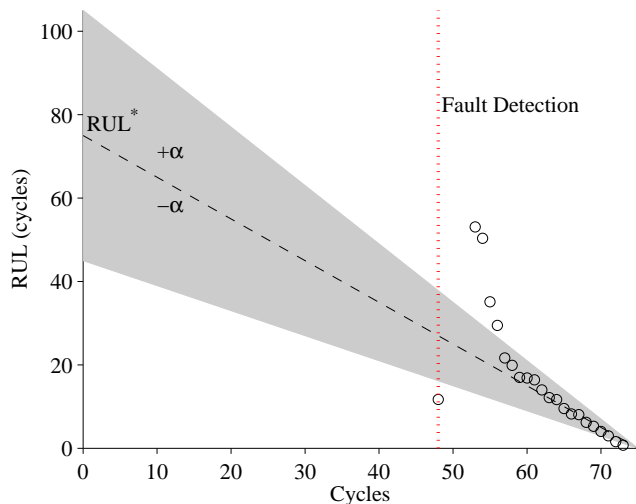


Figure 17. Predicted RUL values for the leak from supply (Exp. 2).

both types of leak faults, thus providing some validation of the approach.

Future work will involve validating the prognosis framework with additional experimental data from the testbed and applying the framework to faults to continuously controlled valves.

#### ACKNOWLEDGMENT

This work was funded in part by the NASA Automated Cryogenic Loading Operations (ACLO) project under the Office of the Chief Technologist (OCT) of Advanced Exploration Systems (AES), and by the Advanced Ground Systems Maintenance (AGSM) Project under the Ground Systems Development and Operations program.

#### REFERENCES

- Balaban, E., Narasimhan, S., Daigle, M., Roychoudhury, I., Sweet, A., Bond, C., & Gorospe, G. (2013). Development of a mobile robot test platform and methods for validation of prognostics-enabled decision making algorithms. *International Journal of Prognostics and Health Management*, 4(1).
- Balaban, E., Saxena, A., Narasimhan, S., Roychoudhury, I., Goebel, K., & Koopmans, M. (2010, September). Airborne electro-mechanical actuator test stand for development of prognostic health management systems. In *Annual conference of the prognostics and health management society 2010*. Portland, OR.
- Daigle, M., & Goebel, K. (2010, March). Model-based prognostics under limited sensing. In *2010 IEEE Aerospace Conference*.
- Daigle, M., & Goebel, K. (2011a, August). A model-based prognostics approach applied to pneumatic valves. *International Journal of Prognostics and Health Management*, 2(2).
- Daigle, M., & Goebel, K. (2011b, March). Prognostics for ground support systems: Case study on pneumatic valves. In *Proceedings of AIAA infotech@aerospace 2011 conference*.
- Daigle, M., & Goebel, K. (2013, May). Model-based prognostics with concurrent damage progression processes. *IEEE Transactions on Systems, Man, and Cybernetics: Systems*, 43(4), 535-546.
- Daigle, M., Kulkarni, C., & Gorospe, G. (2014, March). Application of model-based prognostics to a pneumatic valves testbed. In *Proceedings of the 2014 IEEE aerospace conference*.
- Daigle, M., & Sankararaman, S. (2013, October). Advanced methods for determining prediction uncertainty in model-based prognostics with application to planetary rovers. In *Annual conference of the prognostics and health management society 2013* (p. 262-274).
- Kulkarni, C., Daigle, M., & Goebel, K. (2013, September). Implementation of prognostic methodologies to cryogenic propellant loading testbed. In *IEEE AUTOTEST-CON 2013*.
- Luo, J., Pattipati, K. R., Qiao, L., & Chigusa, S. (2008, September). Model-based prognostic techniques applied to a suspension system. *IEEE Transactions on Systems, Man and Cybernetics, Part A: Systems and Humans*, 38(5), 1156-1168.
- Orchard, M., & Vachtsevanos, G. (2009, June). A particle filtering approach for on-line fault diagnosis and failure prognosis. *Transactions of the Institute of Measurement and Control*(3-4), 221-246.
- Perry, R., & Green, D. (2007). *Perry's chemical engineers' handbook*. McGraw-Hill Professional.
- Poll, S., Patterson-Hine, A., Camisa, J., Garcia, D., Hall, D.,

Lee, C., ... Koutsoukos, X. (2007, May). Advanced diagnostics and prognostics testbed. In *18th international workshop on principles of diagnosis* (pp. 178–185).

Poll, S., Patterson-Hine, A., Camisa, J., Nishikawa, D., Spirkovska, L., Garcia, D., ... Lutz, R. (2007, May). Evaluation, selection, and application of model-based diagnosis tools and approaches. In *AIAA infotech@aerospace 2007 conference and exhibit*.

Tang, L., Hettler, E., Zhang, B., & DeCastro, J. (2011). A testbed for real-time autonomous vehicle phm and contingency management applications. In *Annual conference of the prognostics and health management society 2011*.

Teubert, C., & Daigle, M. (2013, October). I/P transducer application of model-based wear detection and estimation using steady state conditions. In *Proceedings of the annual conference of the prognostics and health management society 2013* (p. 134-140).

## BIOGRAPHIES

**Chetan S. Kulkarni** received the B.E. (Bachelor of Engineering) degree in Electronics and Electrical Engineering from University of Pune, India in 2002 and the M.S. and Ph.D. degrees in Electrical Engineering from Vanderbilt University, Nashville, TN, in 2009 and 2013, respectively. He was a Senior Project Engineer with Honeywell Automation India Limited (HAIL) from 2003 till April 2006. From May 2006 to August 2007 he was a Research Fellow at the Indian Institute of Technology (IIT) Bombay with the Department of Electrical Engineering. From Aug 2007 to Dec 2012, he was a Graduate Research Assistant with the Institute for Software Integrated Systems and Department of Electrical Engineering and Computer Science, Vanderbilt University, Nashville, TN. Since Jan 2013 he has been a Staff Researcher with SGT Inc. at the Prognostics Center of Excellence, NASA Ames Research Center. His current research interests include physics-based modeling, model-based diagnosis and prognosis. Dr. Kulkarni is a member of the Prognostics and Health Management (PHM) Society, AIAA and the IEEE.

**Matthew Daigle** received the B.S. degree in Computer Science and Computer and Systems Engineering from Rensselaer Polytechnic Institute, Troy, NY, in 2004, and the M.S. and Ph.D. degrees in Computer Science from Vanderbilt University, Nashville, TN, in 2006 and 2008, respectively. From September 2004 to May 2008, he was a Graduate Research

Assistant with the Institute for Software Integrated Systems and Department of Electrical Engineering and Computer Science, Vanderbilt University, Nashville, TN. From June 2008 to December 2011, he was an Associate Scientist with the University of California, Santa Cruz, at NASA Ames Research Center. Since January 2012, he has been with NASA Ames Research Center as a Research Computer Scientist. His current research interests include physics-based modeling, model-based diagnosis and prognosis, simulation, and hybrid systems. Dr. Daigle is a member of the Prognostics and Health Management Society and the IEEE.

**George Gorospe** received the B.E. degree in Mechanical Engineering from the University of New Mexico, Albuquerque, New Mexico, USA, in 2012. Since October 2012, he has been a research engineer with the NASA Ames Research Center. His current research interests include mission design, systems engineering, and autonomous mobile robot control and control systems engineering.

**Kai Goebel** received the degree of Diplom-Ingenieur from the Technische Universität München, Germany in 1990. He received the M.S. and Ph.D. from the University of California at Berkeley in 1993 and 1996, respectively.

Dr. Goebel is currently the Technical Area Lead of the Discovery and Systems Health Technology Area at NASA Ames Research Center. He also coordinates the Prognostics Center of Excellence and is the Technical Lead for Prognostics and Decision Making in NASA's System-wide Safety and Assurance Technologies Project. Prior to joining NASA in 2006, he was a Senior Research Scientist at General Electric Corporate Research and Development Center since 1997. He was also an Adjunct Professor of the Computer Science Department at Rensselaer Polytechnic Institute, Troy, NY, between 1998 and 2005 where he taught classes in Soft Computing and Applied Intelligent Reasoning Systems. He has carried out applied research in the areas of real time monitoring, diagnostics, and prognostics and he has fielded numerous applications for aircraft engines, transportation systems, medical systems, and manufacturing systems.

Dr. Goebel holds 15 patents and has co-authored more than 200 technical papers in the field of Systems Health Management. He is currently member of the board of directors of the Prognostics and Health Management Society and Associate Editor of the International Journal of Prognostics and Health Management.